pairs differ considerably (see above). The mean values and the standard deviations of the H-bond length (distances between the heavy atoms, in Å) for the four different classes of H-bonds are as follows: 2.81, 0.06 (n = 13); 2.90, 0.08 (n = 12); 2.91, 0.05 (n = 14); and 2.96, 0.11 (n = 18). The C=O···H—N($tr^2trtr\pi$) H-bond is the shortest, and the N($tr^2trtr\pi$)—H···N($te^2tetete$) one is the longest. The mean value and the standard deviation of H-bond length for all the H-bonds are (in Å) 2.90 and 0.10 (n = 57). The mean values and standard deviations of the X-H···Y (or X···H-Y) angles (in degrees) for the four different types of H-bonds are as follows: 176.8, 2.9 (n = 13); 169.5, 8.8 (n = 12); 177.6, 4.3 (n = 14); and 170.3, 7.3 (n = 18). The mean values and standard deviations of the X-H···Y (or X···H-Y) angles for all the H-bonds are (in degrees) 173.4 and 7.1 (n = 57).

Using the mean values of H-bond lengths and H-bond angles one may construct the geometries of higher oligomers of the DNA base pairs. The stabilization energies of these complexes may be deduced from the values of the electrostatic energy. This approach of estimation of geometries and stabilization energies of DNA base oligomers will be, in our opinion, more accurate than that based on empirical potentials.

V. Conclusions

The nonempirical ab initio SCF method employing the minimal MINI-1 basis set in combination with a London-type expression for the dispersion energy has been applied to all possible DNA base pairs. The following conclusions may be drawn.

(i) Fair agreement between experimental gas-phase enthalpies and theoretical enthalpies at 300 K has been obtained for GC, CC, AT, and TT pairs (experimental values are available only for the pairs mentioned).

(ii) The GC pair, having three H-bonds, is the most stable; the GG pair with just two H-bonds is, however, comparably stable. Furthermore, different pairs with the same types of H-bonds (which are almost linear) may differ considerably in stability. It follows, therefore, that neither the number of H-bonds nor their linearity is primarily responsible for the stability of the pairs. The stability of the pairs is impossible to explain by using only the atoms forming the H-bond; all the atoms of both subsystems must be taken into account.

(iii) The heteropairs are more stable than the homopairs with complementary base pairs; homopairs, on the other hand, are more stable than heteropairs with the noncomplementary base pairs.

(iv) Stabilization energies of different pairs differ greatly; the opposite is true about H-bond lengths.

(v) Formation of all four structures of the AT pair is equally probable; this is true even if the entropy is taken into account.

(vi) Empirical potentials in general fail to predict absolute as well as relative values of stabilization energies. On the other hand, the electrostatic approximation proved to be useful.

(vii) Dispersion energy is responsible for a very important part of total stabilization for all the pairs.

(viii) The basis set superposition error and dispersion energy do not compensate each other; the sum of these terms changes the order of relative stability as predicted by the SCF interaction energy.

(ix) Using the mean values of H-bond lengths and H-bond angles should make it possible to construct the structures of larger DNA base oligomers; their stabilization energies may be estimated on the basis of electrostatic energies.

Registry No. G, 73-40-5; C, 71-30-7; T, 65-71-4; A, 73-24-5.

Theoretical Investigations of the Anaerobic Reduction of Halogenated Alkanes by Cytochrome P450. 1. Structures, Inversion Barriers, and Heats of Formation of Halomethyl Radicals

Brian T. Luke,[†,‡] Gilda H. Loew,*[‡] and A. D. McLean[§]

Contribution from the Molecular Research Institute, Palo Alto, California 94304, SRI International, Menlo Park, California 94025, and IBM Research Laboratory, San Jose, California 95193. *Received June 17, 1985*

Abstract: For understanding the properties of the radicals produced in the anaerobic reduction of halogenated methanes by cytochrome P450, the geometries of all chlorofluoromethyl radicals are optimized with both MNDO and ab initio methods. The ab initio calculations employ unrestricted Hartree–Fock theory with 3-21G and 6-31G* basis sets. In addition, the structures of CH_3, CH_2F, and CH_2Cl are optimized with second-order Møller–Plesset perturbation theory (MP2) with 6-31G*, 6-31G**, and 6-31+G* basis sets. MP2 structures of CH_3 and CH_2F are also obtained with 6-311G** and 6-311+G** basis sets. The degree of nonplanarity, and the inversion barrier, increases in the order H < Cl < F. An examination of the results shows a correlation between the ab initio equilibrium geometry and the inversion barrier for these radicals. A plot of the inversion barrier vs. the degree of nonplanarity produces a single curve for all levels of calculation. This suggests that the equilibrium geometry of the radical determines the magnitude of the inversion barrier. MP2/6-31G*//HF/3-21G energies and HF/3-21G vibrational frequencies of all chlorofluoromethanes and methyl radicals are used with the available experimental data to calculate theoretical heats of formation for these compounds. These theoretical values are used to determine the strengths of C–H bonds in halogenated methanes, which correlate to the activity of the radicals produced in anaerobic reduction toward abstraction of lipid hydrogens. The theoretical heats of formation serve as a guide in deciding between conflicting experimental values. After a reliable set of experimental heats of formation is determined, these values are used to extend the list of HF/3-21G and HF/6-31G* atom equivalents presented by Ibrahim and Schleyer. In addition, MP2/6-31G*//HF/3-21G atom equivalents are determined.

Under anaerobic reducing conditions, various halogenated hydrocarbons are known to be reductively dehalogenated[1] by cytochrome P450. This activity is in contrast to that observed in the presence of O_2 and NADPH, where these heme proteins behave as mixed function oxidases, transfering an oxygen atom from O_2 to a variety of substrates. Initial evidence for this al-

[†] Molecular Research Institute.
[‡] SRI International.
[§] IBM Research Laboratory.

(1) Anders, M. W.; Pohl, L. R. In *Bioactivation of Foreign Compounds*; Anders, M. W., Ed.; Academic: New York, 1985.

0002-7863/87/1509-1307$01.50/0

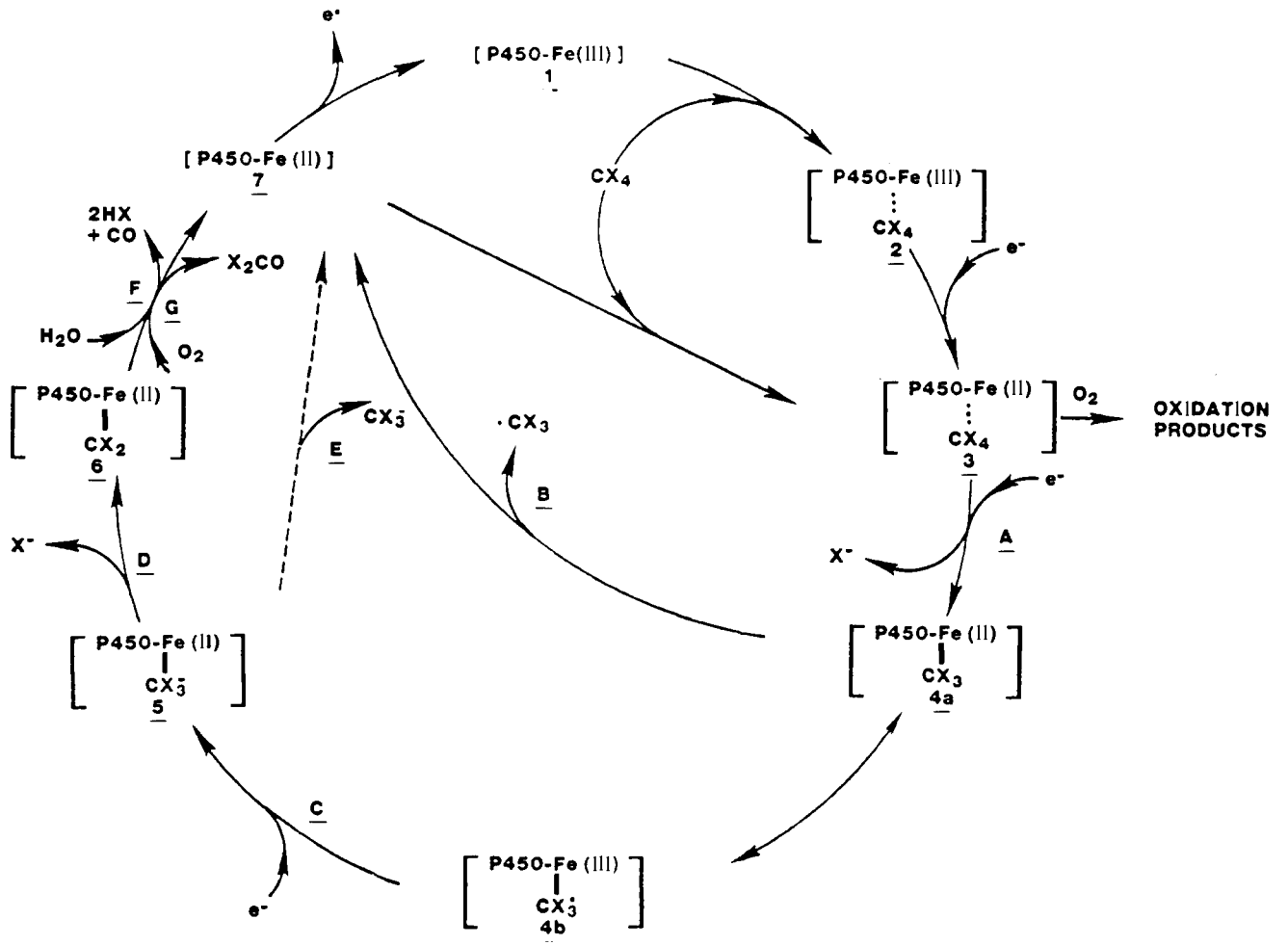

Figure 1. Anaerobic reduction cycle of cytochrome P450.

ternative pathway, presented in Figure 1, stemmed from the observation that, under anaerobic conditions,[2,3] certain halogenated methanes were reductively dehalogenated in the microsomal fraction[4] of renal and hepatic tissue slices and homoginates[5] fortified with NADPH.[6-8] Though this reduction is inhibited by molecular oxygen, it has been suggested that the concentration of O_2 may be quite low in the center of liver lobules.[9] Agents that selectively destroy cytochrome P450 were found to hinder the anaerobic reduction of carbon tetrachloride.[10] It was also shown that a purified reconstituted cytochrome P450 containing system is capable of reductive dehalogenation of CCl_4.[11]

In vivo anaerobic reduction of halocarbons by cytochrome P450 has been linked to the toxic effects of certain anaesthetics, the pesticide DDT, chlorinated alkanes and alkenes, and a number of halomethanes, Experimental investigations have shown that in the first step of the reductive cycle (Figure 1) the halocarbons act as "type I" substrates, They bind to a hydrophobic site of the enzyme **2** that is near, but not attached to, the heme unit.

The second step in this enzymatic cycle is the reduction of the substrate-bound cytochrome P450 by NADPH–cytochrome P450 reductase **3**. Under normal conditions, molecular oxygen would bind to the iron at this stage initiating the transfer of one oxygen atom to various substrates. Instead, if the O_2 concentration is low, a second electron reduction can occur with rapid transfer of an electron to certain halogenated hydrocarbons while in the lipophilic binding site of the enzyme, In this process (reaction A) a halogen anion will be eliminated from halogenated methanes, for example, yielding a halogenated methyl radical.[7,8,12] This radical can either leave the active site of the cytochrome P450 (reaction B) or bind to the iron of the heme group. The species formed can be represented as either a ferrous–haloalkyl radical **4a** or a ferric–carbanion **4b** complex.

Species **4a,b** can accept a third electron forming a ferrous–carbanion complex **5** (reaction C). A recent investigation of the reductive dehalogention of hexachloroethane suggests that this last electron can be transferred by either NADPH–cytochrome P450 reductase or NADH–cytochrome b_5.[3] This ferrous–methyl carbanion complex can eliminate a second halogen anion (reaction D),[13,14] producing a carbene complex. It was also suggested that

(2) (a) Hinsworth, H. P. *The Liver and Its Diseases*; Blackwell: Oxford, 1950. (b) Goldschmidt, S.; Ravdin, I. S.; Lucke, B. *J. Pharmacol.* **1937**, *59*, 1. (c) Strubelt, O.; Breining, H. *Toxic. Lett.* **1980**, *6*, 109. (d) Krishna, G.; Sipes, I. G.; Gilette, J. R. *Pharmacologist* **1973**, *15*, 260. (e) Sipes, I. G.; Krishna, G.; Gilette, J. R. *Life Sci.* **1977**, *20*, 1541. (f) Ahr, H. J.; King, L. J.; Nastaincky, W.; Ullrich, V. *Biochem. Pharmacol.* **1982**, *31*, 383.

(3) Nastalnczky, W.; Ahr, H. J.; Ullrich, V. *Biochem. Pharmacol.* **1982**, *31*, 391.

(4) Wolfe, C. R.; King, L. J.; Parke, D. V. *Chem. Biol. Interact.* **1978**, *21*, 277.

(5) (a) Rubinstein, D.; Kanics, L. *Can. J. Biochem.* **1964**, *42*, 1577. (b) Paul, B. B.; Rubinstein, D. *J. Pharmacol Exp. Ther.* **1963**, *141*, 141.

(6) Slater, T. F.; Sawyer, B. C. *Biochem. J.* **1971**, *123*, 805.

(7) Reiner, O.; Anthanossopoulos, S.; Hellmer, K. H.; Murray, R. E.; Uehleke, H. *Arch. Toxicol.* **1972**, *29*, 219.

(8) Uehleke, H.; Mellmer, K. H.; Tabarelli, S. *Xenobiotica* **1973**, *3*, 1.

(9) Nastainczyk, W.; Ullrich, V.; Seis, H. *Biochem. Pharmacol.* **1978**, *27*, 387.

(10) Recknagel, R. O.; Glende, E. A. *CRC Crit. Rev. Toxicol.* **1973**, *2*, 263. Suarez, K. A.; Bhonsle, P. *Toxicol. Appl. Pharm.* **1976**, *37*, 23.

(11) Wolf, C. R.; Harrelson, W. G.; Nastainczyk, W. M.; Philpot, R. M.; Kalyanaraman, B.; Mason, R. M. *Mol. Pharmacol.* **1980**, *18*, 553.

(12) Fowler, J. S. L. *Br. Pharmacol.* **1969**, *37*, 733.

the methyl carbanion could leave the enzyme (reaction E) and abstract a proton from the solvent.[15] Incubating CCl_4 in anaerobic hepatic microsomal fractions enriched with D_2O yielded no $CDCl_3$, showing that the trichloromethyl carbanion does not leave the cytochrome P450.[14,16]

The carbene–cytochrome P450 complex **6** is responsible for changes in the difference spectrum in the region of 450 nm.[17,18] This carbene may be hydrolyzed to carbon monoxide (reaction F)[14,17,19] or may react with molecular oxygen to form a dihalo carbonyl (reaction G) which can produce toxic effects.

In addition to dihalo carbonyl compounds, the halogenated methyl radicals produced in reaction B are believed to be responsible for the liver damage caused by exposure to various halogenated methanes.[20] Earlier studies on the direct observation of the CCl_3 radical produced from reductive dechlorination of CCl_4 by ESR spectroscopy have proven controversial.[21] Currently, most evidence for such halomethyl radicals comes from the detection of their presumed reaction product.[22] For example, hexachloroethane, believed to be produced from the combination of two CCl_3 radicals, has been identified in tissues[12,23] and incubation mixtures[8] that were treated with CCl_4.

Halomethyl radicals may produce toxicity in two ways. One is by hydrogen abstraction from a lipid molecule to form the corresponding halomethane ($CXZY + LH \rightarrow CHXYZ + L$), an observed major product of anaerobic reduction. The resulting lipid radical (L) can react with molecular oxygen, initiating lipid peroxidation and tissue damage. Alternatively, the halomethyl radical can react with molecular oxygen, a known rapid reaction,[24] to form the halomethyl peroxy radical (X_3COO),[25] another possible metabolite that could cause lipid peroxidation.

Since much of the toxicity of halogenated hydrocarbons can be traced to the formation of haloalkyl radicals during anaerobic reduction by cytochrome P450, it is important to examine these compounds. This paper is the first in a series of theoretical studies designed to investigate the electron-accepting ability of halogenated methanes and ethanes as a determinant of relative substrate efficiency. In particular, this study will examine the structure of the halomethyl radicals produced in reaction B. Since these radicals are also important in atmospheric reactions, the scope of this work has been enlarged. One goal is to examine the equilibrium structure and inversion barrier of all possible chlorofluoromethyl radicals. We will show that there is a definite relationship between the optimized geometry and the height of the inversion barrier and that this correspondence is independent of the basis set or the amount of electron correlation included in the calculation.

Table I. Selected Experimental Heats of Formation (0 K) of the Halogenated Methanes and Methyl Radicals

species	$\Delta H_f°_0$ (reference)	used
CH_4	−15.99 ± 0.08 (68); −15.995 (70, 74)	−16.0
CH_3F	−54 ± 8 (68); −53 ± 2 (69, 75); −54.8 ± 2 (76)	−53.9 ± 2.9
CH_2F_2	−105.9 ± 0.4 (68); −105.4 (69); −105.0 (70); −106.2 ± 1 (76)	−105.6 ± 1.6
CHF_3	−164.9 ± 0.8 (68); −165.1 (69); −162.8 (70); −164.3 ± 1 (76)	−163.95 ± 1.95
CF_4	−221.61 ± 0.3 (68); −220.6 (69); −219.6 (70); −221.6 ± 1 (76)	−220.6 ± 2.0
CH_3Cl	−17.4 (70); −17.7 (69, 75); −18.1 ± 0.5 (77)	−17.75 ± 1.35
CH_2Cl_2	−21.19 ± 0.3 (68); −21.2 (69); −20.46 (70)	−20.83 ± 1.35
$CHCl_3$	−23.48 ± 0.3 (68); −23.42 (69, 70)	−23.45 ± 0.5
CCl_4	−22.42 ± 0.5 (68); −22.4 (69); −24.1 (70)	−23.2 ± 1.35
CH_2FCl	−60.9 ± 3[a] (68); −67.8 (72)	
CHF_2Cl	−113.6 ± 3 (68); −118.4 (72); −110.8 (78)	
$CHFCl_2$	−66.36 ± 3[a] (68); −72.8 (72)	
CF_3Cl	−168.0 ± 0.8 (68); −164.8 (70); −167.8 (79)	
CF_2Cl_2	−116.5 ± 2 (68); −114 ± 2 (69); −113 (70); −117 (79)	
$CFCl_3$	−68.24 ± 1.5 (68); −65.2 (70); −69.2 (79)	
CH_3	35.52 ± 0.2 (68); 35.5 (70); 35.8 ± 0.2 (80, 81)	35.6
CH_2F	−7.0 ± 2 (82, 83)	−7.0 ± 2.0
CHF_2	−58.6 (83, 84)	−58.6 ± 2.0
CF_3	−111.8 ± 1 (68); −111.9 (69); −113.4 (70)	−112.6 ± 1.8
CH_2Cl	30.7 (85); 31.8 (86)	31.25 ± 1.55
$CHCl_2$	26.2 ± 1 (86, 87)	26.2 ± 1.0
CCl_3	18.94 ± 2 (68); 18.44 (69); 13.94 (70); 18.84 ± 0.9 (71)	16.44 ± 3.5
CHFCl	none	
CF_2Cl	−63.9 ± 2 (81)	
$CFCl_2$	−22.7 (88)	

[a] Thermochemical estimate.

The energy of these radicals will also be necessary in the next paper of this series[26] to accurately determine the relative vertical electron affinities of the parent halomethanes. Since it is known that the halomethane resides in a hydrophobic binding site during the reduction process, we can safely assume that the structure of the molecule will be similar to that found in the gas phase. We will also assume that the electron transfer occurs fast enough that the parent halomethane will not be able to relax during this transfer. Therefore, an important indication of whether a halogenated alkane will accept this electron is the magnitude of its vertical electron affinity (VEA). The VEA of these haloalkanes can be calculated in two ways. The first is the direct calculation of the energy change for the reaction

$$CY_3X + e^- \rightarrow CY_3 + X^-$$

A calculation of this energy change will contain significant errors since the reactant is a closed-shell molecule, while one of the products is an open-shell radical. To circumvent this "nonisogyric" problem,[27] we will calculate the energy change for the process

$$CY_3 + X^- \rightarrow CY_3X^-$$

which has open-shell species on both sides of the reaction and should produce a more balanced energy calculation. These results will be used together with experimental values for the enthalpy change for the reaction

$$CY_3X + e^- \rightarrow CY_3 + X^-$$

The VEA is determined from the sum of the energy changes for

(13) Hine, J. *J. Am. Chem. Soc.* **1950**, *37*, 733.
(14) Ahr, H. J.; King, J. L.; Nastainczyk, W.; Ullrich, V. *Biochem. Pharmacol.* **1980**, *29*, 2855.
(15) Ullrich, V.; Schnabel, K. H. *Drug Metab. Dispos.* **1973**, *1*, 173.
(16) Kubic, V. L.; Anders, M. W. *Chem. Biol. Interactions* **1981**, *34*, 201.
(17) (a) Mansuy, D.; Nastainczyk, W.; Ullrich, V. *Arch. Pharmacol.* **1974**, *285*, 315. (b) Wolf, C. R.; Mansuy, D.; Nastainczyk, W.; Ullrich, V. *Biochem. Pharm.* **1978**, *27*, 240.
(18) Mansuy, D. *Pure Appl. Chem.* **1980**, *52*, 681.
(19) (a) Wolf, C. R.; Mansuy, D.; Nastainczyk, W.; Deutschmann, G.; Ullrich, V. *Mol. Pharm.* **1977**, *13*, 698. (b) Harris, R. N.; Anders, M. W. *Fed. Proc.* **1980**, *39*, 611.
(20) (a) Comporti, M.; Benedetti, A. *Biochem. Pharmacol.* **1972**, *21*, 418. (b) Ugazio, G.; Torrielli, V. M. *Biochem. Pharmacol.* **1969**, *18*, 2271. (c) Dianzani, M. U.; Ugazio, G. *Chem. Biol. Interactions* **1973**, *6*, 67. (d) Poyer, J. L.; Floyd, R. A.; McCay, P. B.; Janzen, E. G.; Davis, E. R. *Biochem. Biophys. Acta* **1978**, *539*, 402.
(21) (a) Burdino, E.; Gravela, E.; Ugazio, G.; Vannini, V.; Calligaro, A. *Agents Actions* **1973**, *4*, 244. (b) Calligaro, A.; Vannini, V. *Pharmacol. Res. Commun.* **1975**, *7*, 323. (c) Sancier, K. M. *Pharmacol. Res. Commun.* **1976**, *8*, 429. (d) Calligaro, A.; Vannini, V. *Pharmacol. Rec. Commun.* **1976**, *8*, 431. (e) Mason, R. P. *Rev. Biochem. Toxicol.* **1979**, *1*, 151.
(22) (a) Poyer, J. L.; McCay, P. B.; Lai, E. K.; Janzen, E. G.; Davis, E. R. *Biochem. Biophys. Res. Commun.* **1980**, *94*, 1154. (b) Tomasi, A.; Albino, E.; Lott, K. A. K.; Slater, T. F. *Fed. Eur. Biochem. Soc. Lett.* **1980**, *122*, 303.
(23) Bini, A.; Vecchi, G.; Vivoli, G.; Vannini, V.; Cessi, C. *Pharmacol. Res. Commun.* **1975**, *7*, 143.
(24) (a) Hesse, C.; Leray, N.; Roncin, J. *Mol. Phys.* **1971**, *22*, 137. (b) Packer, J. E.; Willson, R. L.; Bahnemann, D.; Asmus, K. D. *J. Chem. Soc., Perkin Trans. 2*, **1980**, 296.
(25) Packer, J. E.; Slater, T. F.; Wilson, R. L. *Life Sci.* **1978**, *23*, 2617.
(26) Luke, B. T.; Loew, G. H.; McLean, A. D. "Theoretical Investigations of the Anaerobic Reduction of Halogenated Alkanes by Cytochrome P450. 2. Vertical Electron Affinities of Chlorofluoromethanes", in preparation.
(27) Pople, J. A.; Frisch, M. J.; Luke, B. T. Binkley, J. S. *Int. J. Quant. Chem., Quant. Chem. Symp.* **1983**, *17*, 307.

these latter processes, The calculated values of the VEA for all chlorofluoromethanes will be presented in the next paper in this series[26] and will need the energies of the halomethyl radicals presented here.

In addition, we will examine the relative hydrogen abstracting ability of these radicals by determining the strength of the resulting CX_3–H bond. The simplest method of calculating the strength of the C–H bond in halogenated methanes would be to use experimental heats of formation of the halogenated methyl radical and its hydrogenated methane analogue. This also corresponds to the maximum strength of a bond that a given radical can cleave during hydrogen abstraction from a lipid carbon (C_L–H). The available experimental heats of formation for these species are presented in Table I. This table shows that no experimental data are available for one of the radicals (CHFCl) and that there are a wide range of values for several other species. Therefore, these data are not sufficient to determine accurate C–H bond strengths. By theoretically calculating the energy change for a series of reactions and using the accurate heats of formation of CH_4 and CH_3, the heat of formation of any other species can be determined. For example, all fluorine substituted methyl radicals and methanes can be formed from CH_3F from the reactions

$$CH_3 + nCH_3F \rightarrow nCH_4 + CH_{3-n}F_n \quad (1a)$$

$$nCH_3F \rightarrow (n-1)CH_4 + CH_{4-n}F_n \quad (1b)$$

If the heat of formation of CH_3F was accurately known, the calculated energies for the above reactions could be used to determine $\Delta H_f°_0$ for all other species. Unfortunately, an experimental uncertainty of 2 kcal/mol in the heat of formation of CH_3F would translate into an additional uncertainty of 8 kcal/mol in CF_4.

To reduce the spread in the experimental heats of formation, we theoretically determine the energy change for reactions 1 and the corresponding reactions where chlorine is substituted for fluorine. These calculated reaction energies are used to determine theoretical heats of formation for CH_3F and CH_3Cl. These values are then used to calculate the heat of formation of all other halomethanes and methyl radicals and the C–H bond strength in the halogenated methanes. The stronger this bond, the better the radical will be at hydrogen abstraction from different chemical environments.

There has been some experimental controversy over the degree of nonplanarity in these chlorofluoromethyl radicals. Three factors will qualitatively control the structure of these molecules. One of these is an interaction between the unpaired electron on the carbon and the nonbonding electrons of the halogen in the planar conformation. Bernardi and co-workers[28,29] have shown that a 2-orbital, 3-electron interaction (as would be found in CH_2X) may either stabilize or destabilize the planar conformation. Two or more halogen atoms bound to the radical carbon will cause the molecule to prefer a nonplanar geometry,[30,31] though this effect will decrease with increasing carbon–halogen separations.

There is also an electrostatic repulsion between the halogen atoms, resulting in a longer bond length in the nonplanar structure and a preference for a planar geometry. This effect will decrease in the order F, Cl, Br, I, since the carbon–halogen bond length increases and the electronegativity of the halogen, and its resulting partial charge decreases.

The third factor is the hybridization change of the central carbon. In the nonplanar structure the carbon has approximately sp^3 hybridization; in the planar structure it is approximately sp^2. The change from sp^3 to sp^2 will lower the energy of the carbon–halogen bonding orbitals (due to a higher percentage of s-character) and will raise the energy of the orbital containing the unpaired electron.

The first two effects generally work in opposite directions and both will decrease with increasing carbon–halogen separations, so there is no a priori way to predict the geometry of these radicals. What can be said is that both the first and third factors will cause the geometry to become more nonplanar if two unpaired electrons reside on the central atom. Therefore, the geometry of the halogenated methyl radical should be more planar than the corresponding carbanion.

This study examines the effect of halogen substitution on the equilibrium structure of the methyl radical and the C–H bond strength in halomethanes. The optimized geometries of CH_3 and all possible F- and Cl-substituted radicals (CH_2F, CHF_2, CF_3, CH_2Cl, $CHCl_2$, CCl_3, CHFCl, CF_2Cl, and $CFCl_2$) are determined with ab initio[32] and MNDO[33] methods. The next section outlines the computational methods used and is followed by a detailed presentation and discussion of the results.

Method of Computation

In an earlier study of saturated first- and second-row amines,[34] it was shown that polarization functions on the nitrogen were necessary to properly describe the geometry and inversion barriers about the nitrogen. Therefore, the ab initio calculations described here were preformed with use of two different basis sets: the 3-21G basis,[35] and the 6-31G* basis[36] which includes a set of six Cartesian d-functions on all non-hydrogen atoms. All geometries were optimized with Unrestricted Hartree–Fock (UHF) theory[37] theory for both ab initio and MNDO calculations. If the molecule was found to have a nonplanar equilibrium conformation, the geometry of the planar transition structure for inversion was also determined.

To assess the effects of including electron correlation on the structure, the geometries of CH_3, CH_2F, and CH_2Cl were optimized with second-order Møller–Plesset perturbation theory (MP2),[38] with the 6-31G* and 6-31G** basis sets.[36] This latter basis includes p-functions on all hydrogen atoms. In addition, MP2 optimizations were also determined with the 6-31+G* and 6-31+G** basis sets,[39] which contain diffuses s- and p-functions on all non-hydrogen atoms. For CH_3 and CH_2F, MP2 geometries were also obtained with the 6-311G**[40] and 6-311+G** basis sets. Since CH_2Cl and CH_2F were found to have slightly nonplanar equilibrium structures, values of the inversion barrier were determined at higher levels of theory by performing single-point calculations with full fourth-order Møller–Plesset perturbation theory (MP4SDTQ)[41] at all optimized structures with the 6-31++G** basis for CH_2Cl and the 6-31++G** and 6-311++G** basis sets for CH_2F. These basis sets include polarization and diffuse functions on all atoms.

Calculations of the energy change for reactions 1a and 1b are performed at the MP2/6-31G*//HF/3-21G level of theory,[26] where the level of calculation used to determine the total energy is given to the left of the "//" and the method used to optimize the geometry is given to the right. The change in the zero-point vibrational energy for each reaction is determined by calculating the HF/3-21G harmonic frequencies and the zero-point energy of each species. Before they are combined to produce the vi-

(28) Bernardi, F.; Epiotis, N. D.; Cherry, W.; Schlegel, H. B.; Whangbo, M. H.; Wolfe, S. *J. Am. Chem. Soc.* **1976**, *98*, 4969.
(29) Bernardi, F.; Cherry, W.; Shaik, S.; Epiotis, N. D. *J. Am. Chem. Soc.* **1978**, *100*, 1352.
(30) Bingham, R. C.; Dewar, M. J. S. *J. Am. Chem. Soc.* **1973**, *95*, 7182.
(31) Krusic, P. J.; Bingham, R. C. *J. Am. Chem. Soc.* **1976**, *98*, 230.
(32) Binkley, J. S.; Frisch, M.; DeFrees, D. J.; Ragavachari, K.; Whiteside, R. A.; Schlegel, H. B.; Flueter, G.; Pople, J. A., Carnegie-Mellon Chemistry Publication Unit, 1983.
(33) Stewart, J. P. *Quantum Chemistry Program Exchange* Department of Chemistry, Indiana University, Bloomington, Indiana 47405; No. 455., MOPAC (Version 2.0).
(34) Luke, B. T.; Pople, J. A. "Ab Initio Calculations of the Structures of First- and Second-Row Amines", in preparation.
(35) (a) Binkley, J. S.; Pople, J. A.; Hehre, W. J. *J. Am. Chem. Soc.* **1980**, *102*, 939. (b) Gordon, M. S.; Binkley, J. S.; Pople, J. A.; Pietro, W. J.; Hehre, W. J. *J. Am. Chem. Soc.* **1982**, *104*, 2792.
(36) Hariharan, P. C.; Pople, J. A. *Theor. Chim. Acta* **1973**, *28*, 213.
(37) Pople, J. A.; Nesbet, R. K. *J. Chem. Phys.* **1954**, *22*, 541.
(38) Binkley, J. S.; Pople, J. A. *Int. J. Quant. Chem.* **1975**, *9*, 229.
(39) Frisch, M. J.; Pople, J. A.; Binkley, J. S. *J. Chem. Phys.* **1984**, *80*, 3265.
(40) Krishnan, R.; Binkley, J. S.; Seeger, R.; Pople, J. A. *J. Chem. Phys.* **1980**, *72*, 650.
(41) (a) Krishnan, R.; Pople, J. A. *Int. J. Quant. Chem.* **1978**, *14*, 91. (b) Krishnan, R.; Frisch, M. J.; Pople, J. A. *J. Chem. Phys.* **1980**, *72*, 4244.

Table II. Optimized Equilibrium Geometries of the Planar CH_3 Radical

level	r(C-H)[a]	energy[b]
MNDO	1.078	24.6
HF/3-21G	1.072	-39.342 61
HF/6-31G*	1.073	-39.558 99
MP2/6-31G*	1.079	-39.668 75
MP2/6-31G*	1.080	-39.672 41
MP2/6-31G**	1.074	-39.692 70
MP2/6-31+G**	1.075	-39.696 33
MP2/6-311G**	1.079	-39.707 24
MP2/6-311+G**	1.080	-39.708 53

[a] Bond length is in angstroms. [b] Energy is in kcal/mol for MNDO and hartrees for the ab initio methods.

brational contribution of the reaction energy, each zero-point energy is scaled by a factor which was determined from an extensive comparison of calculated and experimental zero-point energies.[42]

Since the same number of each type of chemical bond is present in the reactants and products of reactions 1, these reactions are termed isodesmic.[43] In addition, the carbon atom in reaction 1b always retains sp^3 hybridization, producing a set of homodesmic reactions.[43b] All halomethyl radicals are found to have nonplanar equilibrium geometries, suggesting that the central carbon has at least partial sp^3 hybridization. This would also make reaction 1a homodesmic. Earlier studies[43] have shown that calculations of iso- and homodesmic reactions yield accurate reaction energies, and since we are including some electron correlation, we expect the resulting energies to be accurate to within 2 kcal/mol.

In the last column of Table I, we have listed an experimental heat of formation and errors that incompass all of the previously reported values for the fluorinated and chlorinated methanes and methyl radicals. From each heat of formation and error, and an assumed calculated error of 2 kcal/mol, we obtain a range of values for the heat of formation of CH_3F and CH_3Cl. By taking an intersection of these ranges, we can determine a range of values for these heats of formation that satisfy most or all of these reactions. Once a heat of formation of CH_3F and CH_3Cl is determined, all other heats of formation are calculated.

Results

The methyl radical, CH_3, is predicted to be planar at all levels of calculation (Table II). Previous ab initio results using large basis sets[44] also obtained a planar geometry, while INDO[45,46] and minimum basis set ab initio calculations[47,48] produced slightly nonplanar structures. The inclusion of electron correlation with the 6-31G* basis produces an increase in the equilibrium C-H separation of 0.006 Å. For all nondiffuse basis sets, the addition of diffuse s- and p-functions on the central carbon slightly increases the internuclear separation. Adding polarization functions to the hydrogen atoms decreased the C-H separation, while adding a third set of valence s- and p-functions increased the C-H bond length.

There is some experimental evidence that thermal agitation causes slight nonplanarity,[49] though Ellison and co-workers[50] predict that the barrier is less than half of the corresponding zero-point vibrational energy. Hirota and co-workers[51,52] examined the spectra of CH_3 and concluded that there is no hump in the potential energy surface at a planar geometry, but there is a large negative anharmonicity for the out-of-plane bending motion. All calculated equilibrium structures are in good agreement with experiment.[53]

Table III. Optimized Equilibrium Structures of the CH_2F Radical[a]

level	r(C-F)	r(C-H)	θ(H-C-F)	θ(H-C-H)	β
MNDO	1.305	1.086	118.6	122.8	90.0
HF/3-21G	1.367	1.069	115.3	122.5	98.8
HF/6-31G*	1.331	1.073	113.9	121.2	101.1
MP2/6-31G*	1.352	1.082	114.2	122.0	100.4
MP2/6-31+G*	1.361	1.081	113.4	123.3	100.5
MP2/6-31G**	1.350	1.078	114.3	121.9	100.4
MP2/6-31+G**	1.360	1.078	113.5	123.2	100.5
MP2/6-311G**	1.341	1.081	113.5	122.7	99.8
MP2/6-311+G**	1.344	1.081	114.1	123.3	99.7

[a] Bond lengths are in angstroms, angles are in degrees.

Table IV. Optimized Structures of the Planar CH_2F Radical[a]

level	r(C-F)	r(C-H)	θ(H-C-F)
MNDO	1.305	1.086	118.6
HF/3-21G	1.365	1.065	116.8
HF/6-31G*	1.328	1.068	116.4
MP2/6-31G*	1.349	1.077	116.4
MP2/6-31+G*	1.357	1.073	115.7
MP2/6-31G**	1.347	1.076	116.5
MP2/6-31+G**	1.356	1.073	115.7
MP2/6-311G**	1.338	1.076	116.3
MP2/6-311+G**	1.341	1.076	116.0

[a] Bond lengths are in angstroms, angles are in degrees.

Table V. Ab Initio Total Energies of the Equilibrium (C_s) and Planar (C_{2v}) Structures of CH_2F and the Magnitude of the Inversion Barrier Calculated at the Level of Optimization and the MP4SDTQ Level with the 6-31++G** and 6-311++G** Basis Sets[a]

level	C_s	C_{2v}	ΔE
Optimization Level			
HF/3-21G	-137.652 64	-137.651 90	0.5
HF/6-31G*	-138.402 11	-138.400 08	1.3
MP2/6-31G*	-138.679 29	-138.677 89	0.9
MP2/6-31G*	-138.695 39	-138.694 01	0.9
MP2/6-31G**	-138.695 52	-138.694 11	0.9
MP2/6-31+G**	-138.711 37	-138.710 00	0.9
MP2/6-311G**	-138.773 03	-138.771 96	0.7
MP2/6-311+G**	-138.781 49	-138.780 50	0.6
MP4SDTQ/6-31++G**			
HF/3-21G	-138.736 40	-138.735 21	0.7
HF/6-31G*	-138.735 86	-138.734 66	0.8
MP2/6-31G*	-138.736 68	-138.735 38	0.8
MP2/6-31G*	-138.736 80	-138.735 49	0.8
MP2/6-31G**	-138.736 64	-138.735 34	0.8
MP2/6-31+G**	-138.736 79	-138.735 47	0.8
MP2/6-311G**	-138.736 39	-138.735 13	0.8
MP2/6-311+G**	-138.736 53	-138.735 23	0.8
MP4SDTQ/6-311++G**			
HF/3-21G	-138.807 24	-138.806 35	0.6
HF/6-31G*	-138.807 39	-138.806 61	0.5
MP2/6-31G*	-138.807 91	-138.807 00	0.6
MP2/6-31G*	-138.807 82	-138.806 92	0.6
MP2/6-31G**	-138.807 86	-138.806 94	0.6
MP2/6-31+G**	-138.807 79	-138.806 89	0.6
MP2/6-311G**	-138.807 83	-138.806 97	0.5
MP2/6-311+G**	-138.807 94	-138.807 00	0.6

[a] Total energies are in hartrees, inversion barriers in kcal/mol.

(42) Pople, J. A.; Schlegel, H. B.; Krishnan, R.; DeFrees, D. J.; Binkley, J. S.; Frisch, M. J.; Whiteside, R. A.; Hout, R. J.; Hehre, W. J. *Int. J. Quant. Chem. Symp.* **1981**, *S15*, 269.
(43) (a) Hehre, W. J.; Ditchfield, R.; Radom, L.; Pople, J. A. *J. Am. Chem. Soc.* **1970**, *92*, 4796. (b) George, P.; Trachtman, M.; Brett, A. M.; Brock, C. W. *J. Chem. Soc., Perkin Trans. 2* **1977**, 1036.
(44) (a) DeFrees, D. J.; Levi, B. A.; Pollack, S. K.; Hehre, W. J.; Binkley, J. S.; Pople, J. A. *J. Am. Chem. Soc.* **1979**, *101*, 4085. (b) Botschwina, P.; Flesch, J.; Meyer, W. *Chem. Phys.* **1983**, *74*, 321.
(45) Beveridge, D. L.; Dobosh, P. A.; Pople, J. A. *J. Chem. Phys.* **1968**, *48*, 4802.
(46) Biddles, I.; Hudson, A. *Mol. Phys.* **1973**, *25*, 707.
(47) Lathan, W. A.; Hehre, W. J.; Curtiss, L. A.; Pople, J. A. *J. Am. Chem. Soc.* **1971**, *93*, 6377.
(48) Aarons, L. J.; Hiller, I. H.; Guest, M. F. *J. Chem. Soc., Faraday Trans. 2* **1974**, *70*, 167.
(49) Koenig, T.; Balle, T.; Snell, W. *J. Am. Chem. Soc.* **1975**, *97*, 662.
(50) Ellison, G. B.; Engelking, P. C.; Lineberger, W. C. *J. Am. Chem. Soc.* **1978**, *100*, 2556.
(51) Yamada, C.; Hirota, E.; Kawaguchi, K. *J. Chem. Phys.* **1981**, *75*, 5256.
(52) Hirota, E. *J. Phys. Chem.* 1983, *87*, 3375.

Table VI. Optimized Equilibrium Structures of the CH_2Cl Radical[a]

level	r(C-Cl)	r(C-H)	θ(H-C-Cl)	θ(H-C-H)	β
MNDO	1.724	1.076	117.9	124.2	90.0
HF/3-21G	1.824	1.067	114.4	125.5	97.9
HF/6-31G*	1.718	1.070	116.5	122.3	97.2
MP2/6-31G*	1.702	1.078	117.4	122.8	95.1
MP2/6-31+G*	1.701	1.078	117.7	123.7	95.2
MP2/6-31G**	1.700	1.074	117.4	122.7	93.1
MP2/6-31+G**	1.700	1.074	117.7	123.6	93.2

[a] Bond lengths are in angstroms, angles are in degrees.

The optimized equilibrium structure of the CH_2F radical at all levels of theory is presented in Table III. Along with bond lengths and interatomic angles, an extra angle, denoted β, is included for all nonplanar structures. This is the angle to the line through the carbon atom which makes an equal angle with all bonds; for CX_3 molecules, it is the angle to the C_{3v} axis. The value of β is expected to lie between 90° (the value for the planar structure) and 109.5° (representing a regular tetrahedral geometry).

Since all levels of theory, except MNDO, predict CH_2F to have a nonplanar equilibrium structure, the planar conformation was also optimized. These results are presented in Table IV. The calculated energies, both at the level of optimization and from single-point calculations at the MP4SDTQ/6-31++G** and MP4SDTQ/6-311++G** levels, along with the magnitude of the inversion barrier are listed in Table V. Including electron correlation with the 6-31G* basis increases the C-F and C-H bond lengths for both the nonplanar and planar equilibrium structures. This increase in the bond lengths is possibly responsible for a decrease in the nonplanarity (β value) of the equilibrium structure, which causes a decrease in the inversion barrier. Adding diffuse functions to non-hydrogen atoms in the 6-31G* basis further increases the C-F separation, but causes virtually no change in the nonplanarity of the equilibrium structure or the inversion barrier. Adding polarization functions to the hydrogen atoms decreases the C-H distance in the equilibrium structure, but it does not affect the degree of nonplanarity or the inversion barrier. Increasing the number of valence orbitals decreases the C-F bond length, as well as the degree of nonplanarity and the inversion barrier. Adding diffuse functions to this 6-311G** basis causes little change in the geometry or the inversion barrier.

The MP4SDTQ/6-31++G** single-point calculations appears to show a stabilization of the inversion barrier at approximately 0.8 kcal/mol. By looking at the total energy of each optimized structure, the MP2/6-31+G* geometry seems to be closest to what would be the MP4SDTQ/6-31++G** optimized structure for both the nonplanar equilibrium structure and the planar transition structure. The MP4SDTQ/6-311++G** calculations also appear to stabilize the inversion barrier at a slightly lower value of 0.6 kcal/mol. By again looking at the total energies, the MP2/6-311+G** equilibrium structure seems to be closest to what would be obtained if the molecule were optimized at the MP4SDTQ/6-311++G** level, while both the MP2/6-31G* and MP2/6-311+G** structures for the planar conformation yield the lowest total energy at the MP4SDTQ/6-311++G** level. It is interesting to note that the HF/3-21G and HF/6-31G* values of the inversion barrier bracket the barriers found at all other levels of theory. As the level of the calculation increases, the inversion barrier approaches the lower HF/3-21G value.

Earlier ab initio[28,54-56] and INDO[45,46] calculations also show a nonplanar equilibrium structure for CH_2F. These results suggest that the experimental geometry of CH_2F will probably appear planar, though a detailed analysis of the vibrational energies for inversional motion should indicate a slight maximum in the potential surface. Though the laser magnetic resonance study of

Table VII. Optimized Structures of the Planar CH_2Cl Radical[a]

level	r(C-Cl)	r(C-H)	θ(H-C-Cl)
MNDO	1.724	1.076	117.9
HF/3-21G	1.816	1.065	115.9
HF/6-31G*	1.714	1.069	117.8
MP2/6-31G*	1.700	1.077	118.0
MP2/6-31+G*	1.700	1.078	118.0
MP2/6-31G**	1.699	1.073	118.1
MP2/6-31+G**	1.699	1.074	118.0

[a] Bond lengths are in angstroms, angles are in degrees.

Table VIII. Ab Initio Total Energies of the Equilibrium (C_s) and Planar (C_{2v}) Structures of CH_2Cl and the Magnitude of the Inversion Barrier Calculated at the Level of Optimization and the MP4SDTQ Level with the 6-31++G** Basis Set[a]

level	C_s	C_{2v}	ΔE
Optimization Level			
HF/3-21G	-496.052 51	-496.052 19	0.2
HF/6-31G*	-498.461 08	-498.460 81	0.2
MP2/6-31G*	-498.697 96	-498.697 89	0.0
MP2/6-31+G*	-498.702 20	-498.702 19	0.0
MP2/6-31G**	-498.713 79	-498.713 72	0.0
MP2/6-31+G**	-498.718 00	-498.717 98	0.0
MP4SDTQ/6-31++G**			
HF/3-21G	-498.747 25	-498.747 54	-0.2
HF/6-31G*	-498.752 28	-498.752 43	-0.1
MP2/6-31G*	-498.752 47	-498.752 50	0.0
MP2/6-31+G*	-498.752 50	-498.752 49	0.0
MP2/6-31G**	-498.752 45	-498.752 48	0.0
MP2/6-31+G**	-498.752 49	-498.752 48	0.0

[a] Total energies are in hartrees, inversion barriers in kcal/mol.

Mucha and co-workers[57] suggested that CH_2F has a planar equilibrium structure, recent experimental evidence[52,58] supports the prediction of a slight hump in the potential surface at a planar geometry.

The optimized equilibrium structure of the CH_2Cl radical is presented in Table VI for each level of theory examined. Again all levels predict that this radical will have a nonplanar equilibrium conformation, with the exception of MNDO. The optimized geometry of the planar structure is given in Table VII, while the ab initio energies of each species and the inversion barriers are listed in Table VIII. Including electron correlation with the 6-31G* basis reduces the C-Cl bond length and produces a slightly more planar equilibrium structure. The C-Cl separation and degree of nonplanarity decreases further when polarization functions are added to the hydrogen atoms, though adding diffuse functions to either the 6-31G* or 6-31G** basis sets causes virtually no change in the geometry or the inversion barrier. The MP2/6-31G** and MP2/6-31+G** equilibrium structures have only a small degree of nonplanarity (their β values are 93.1 and 93.2°, respectively), yielding inversion barriers that are less than 0.05 kcal/mol.

Single-point calculations at the MP4SDTQ/6-31++G** level of theory predict that the planar structure is more stable than the nonplanar conformation for all but the MP2/6-31+G* and MP2/6-31+G** optimizations. The nonplanar structure with the lowest MP4SDTQ/6-31++G** total energy is the MP2/6-31+G* geometry, while the MP2/6-31G* planar structure gave the lowest energy of the planar conformations. Since the MP4SDTQ/6-31++G** energy is identical for these structures, the levels of theory presented here are not able to conclusively determine if the CH_2Cl molecule has a planar or nonplanar equilibrium structure. If it is nonplanar, its degree of nonplanarity is expected to be small, and the inversion barrier should be less than 0.1 kcal/mol. Unlike the case for CH_2F, both the HF/3-21G and HF/6-31G* calculations slightly overestimated the inversion

(53) Herzberg, G. *Proc. R. Soc.* **1961**, *A262*, 291.
(54) Morokuma, K.; Pedersen, L.; Karplus, M. *J. Chem. Phys.* **1968**, *48*, 4801.
(55) Lathan, W. A.; Curtiss, L. A.; Hehre, W. J.; Lisle, J. B.; Pople, J. A. *Prog. Phys. Org. Chem.* **1974**, *11*, 175.
(56) Leroy, G.; Peeters, D. *J. Mol. Struct.* **1981**, *85*, 133.
(57) Mucha, J. A.; Jennings, D. A.; Evenson, K.; Hougen, J. T. *J. Mol. Spectrosc.* **1977**, *68*, 122.
(58) Endo, Y.; Yamada, C.; Saito, S.; Hirota, E. *J. Chem. Phys.* **1983**, *79*, 1605.

Table IX. MNDO, HF/3-21G, and HF/6-31G* Optimized Geometries of F- and Cl-Substituted Methyl Radicals[a]

molecule	symmetry	parameter	MNDO	HF/3-21G	HF/6-31G*
CHF_2	C_s	r(C-F)	1.310	1.346	1.314
		r(C-H)	1.088	1.069	1.076
		θ(H-C-F)	122.2	114.9	113.8
		θ(F-C-F)	113.0	111.9	111.1
		β	95.3	104.6	105.8
CHF_2	C_{2v}	r(C-F)	1.309	1.341	1.310
		r(C-H)	1.085	1.059	1.063
		θ(H-C-F)	123.3	122.5	122.6
CF_3	C_{3v}	r(C-F)	1,312	1,329	1.301
		θ(F-C-F)	115.4	111.6	111.3
		β	102.7	107,2	107,6
CF_3	D_{3h}	r(C-F)	1.300	1.328	1.300
$CHCl_2$	C_s	r(C-Cl)		1.800	1.712
		r(C-H)		1.067	1.070
		θ(H-C-Cl)		116.3	116.4
		θ(Cl-C-Cl)		116.4	118.7
		β		101,2	99.8
$CHCl_2$	C_{2v}	r(C-Cl)	1,716	1.786	1.702
		r(C-H)	1.077	1.065	1.068
		θ(H-C-Cl)	120.0	120.8	119.7
CCl_3	C_{3v}	r(C-Cl)		1.793	1.714
		θ(Cl-C-Cl)		116.3	117.1
		β		101.2	99.8
CCl_3	D_{3h}	r(C-Cl)	1.711	1.777	1.702
CHFCl	C_1	r(C-F)		1.344	1.317
		r(C-Cl)		1.828	1.720
		r(C-H)		1.068	1.073
		θ(F-C-Cl)		113,3	113.9
		θ(F-C-H)		116.6	114.1
		θ(Cl-C-H)		113,3	115.9
		β		103.9	103.6
CHFCl	C_s	r(C-F)	1.298	1,343	1.316
		r(C-Cl)	1.738	1.793	1.696
		r(C-H)	1.083	1.063	1.066
		θ(F-C-Cl)	118.9	116.5	117.1
		θ(F-C-H)	121.8	122.1	119.2
CF_2Cl	C_s	r(C-F)	1.308	1.329	1.303
		r(C-Cl)	1,756	1.832	1.725
		θ(Cl-C-F)	119.2	112.8	113.6
		θ(F-C-F)	112.7	111.9	110.6
		β	100.1	106.2	106.1
CF_2Cl	C_{2v}	r(C-F)	1,303	1,336	1.305
		r(C-Cl)	1.723	1.774	1.681
		θ(Cl-C-F)	122.4	121.2	122.0
$CFCl_2$	C_s	r(C-F)	1,296	1.333	1.309
		r(C-Cl)	1,738	1.811	1.718
		θ(F-C-Cl)	118.8	113.2	112.9
		θ(Cl-C-Cl)	117.9	115.2	117.7
		β	97.2	104.6	103.8
$CFCl_2$	C_{2v}	r(C-F)	1.295	1.336	1.312
		r(C-Cl)	1.726	1.780	1.692
		θ(F-C-Cl)	120.2	119.0	117.7

[a] Bond lengths are in angstroms, angles in degrees.

barrier, though this may not be incorrect in predicting a nonplanar equilibrium structure.

Table IX contains the MNDO, HF/3-21G, and HF/6-31G* optimized geometries of all other F- and Cl-substituted methyl radicals. The optimized energies and resulting inversion barriers are shown in Table X for each species. Molino and co-workers[59] have previously published the MNDO optimized geometries of many of these species, though the structures of CHFCl and $CFCl_2$ in Table IX are new results. All methods of calculation show that the degree of nonplanarity increases as the hydrogens in CH_3 are successively replaced by fluorines.

In agreement with earlier semiempirical[45,46,59,60] and ab initio[29,56,60,61] results, the CHF_2 molecule is predicted to be nonplanar at all levels of calculation. The inversion barrier and degree of nonplanarity of the equilibrium structure increases in the order MNDO, HF/3-21G, HF/6-31G*. The ab initio calculations show a significant decrease in the C-F separation between CH_2F and CHF_2 and only a slight change in the C-H bond length. There is also a larger decrease in all bond lengths when the equilibrium structure becomes planar in CHF_2 than is found in CH_2F. The inversion barrier calculated at the ab initio levels is larger than that found in NH_3 with use of the same basis sets.[34] The HF/3-21G inversion barrier is 1,0 kcal/mol larger than that found with use of the STO-3G basis set,[61] and the same as that reported in an earlier HF/4-31G calculation.[29] The HF/6-31G* barrier is 3.2 kcal/mol larger than the HF/3-21G value, though if the above-mentioned results for CH_2F also apply for CHF_2, the true inversion barrier may be closer to the lower HF/3-21G value of 6.8 kcal/mol. These results support the experimental conclusion[31] that CHF_2 is significantly more nonplanar than CH_2F, obtained by analyzing the ESR hyperfine splittings.

The CF_3 radical has already received a great deal of theoretical attention.[29,45,46,48,54,59-63] All calculational methods except MINDO/3[62] agree with experiment[64,65] in finding CF_3 to be nonplanar. The degree of nonplanarity and the inversion barrier again increase in the order MNDO, HF/3-21G, HF/6-31G*, with the HF/6-31G* F-C-F angle being in closest agreement with experiment. This experimental F-C-F angle (110.7°)[65] corresponds to a β value of 108.2°, suggesting a slightly greater degree of nonplanarity than is calculated here. The HF/STO-3G inversion barrier[61] again lies between the MNDO and HF/3-21G values, while the HF/4-31G barrier[29] is 1.2 kcal/mol less than the HF/3-21G value. Virtually no change is found in the C-F separation when the equilibrium structure becomes planar at the HF/3-21G and HF/6-31G* levels.

In $CHCl_2$, both ab initio calculations predict a nonplanar equilibrium structure while the MNDO method yields a planar geometry. Previously reported INDO[28] and HF/4-31G[60] calculations also predict a nonplanar equilibrium molecule. The inversion barrier is 1,2 and 0,9 kcal/mol at HF/3-21G and HF/6-31G*, respectively. The HF/3-21G results suggest that the inversion barrier for $CHCl_2$ lies between that of CH_2F and CHF_2 while the HF/6-31G* results predict that the inversion barrier for $CHCl_2$ is less than that of CH_2F. The values of β follow the same trends. The extended calculations on CH_2Cl suggest that the true inversion barrier for $CHCl_2$ may be less than 0,9 kcal/mol. The C-Cl and C-H bond lengths are shorter in the transition structure than in the equilibrium geometry for both basis sets.

While early experimental studies suggested that the CCl_3 molecule may have a planar equilibrium structure,[66] later studies have shown a pyramidal equilibrium structure.[67] Earlier INDO[46] and minimum basis set ab initio[48] calculations yielded a nonplanar molecule. In this study, the CCl_3 radical is predicted to have the same degree of nonplanarity (same β value) as $CHCl_2$ at both

(59) Molino, L. M.; Poblett, J. M.; Canadell, E. *J. Chem. Soc., Perkin Trans. 2* **1982**, 1217.

(60) Baird, N. C. *Can. J. Chem.* **1983**, *61*, 1567.
(61) Leroy, G.; Peeters, D.; Wilante, C.; Khalil, M. *Nouv. J. Chim.* **1980**, *4*, 403.
(62) Bischof, P. *J. Am, Chem. Soc.* **1976**, *98*, 6844.
(63) Washlda, N.; Suto, M.; Nagase, S.; Nagashima, U.; Morokuma, K, *J. Chem. Phys*, **1983**, *78*, 1025,
(64) (a) Fessenden, R. W.; Schuler, R. H. *J. Chem. Phys.* **1965**, *43*, 2704. (b) Fessenden, R. W. *J. Phys. Chem.* **1967**, *71*, 74. (c) Endo, Y.; Yamada, C.; Saito, S.; Hirota, E. *J. Chem. Phys.* **1982**, *77*, 3376.
(65) Yamada, C.; Hirota, E. *J. Chem. Phys*, **1981**, *78*, 1703.
(66) (a) Magat, M.; Leroy, N.; Roncln, J. Mater. Nauchns-Tekh. Konf.-*Vses. Khim. O-vs. im. D. I. Mendeleeva Tatar. Resp. Pravl.* **1966**, *11*, 233. (b) Rogers, E. E.; Abramowitz, S.; Jacox, M. E.; Milligan, D. E. *J. Chem. Phys.* **1970**, *52*, 2198.
(67) (a) Andrews, L. *J. Phys. Chem.* **1967**, *71*, 2761. (b) Andrews, L. *J. Chem. Phys.* **1968**, *48*, 972. (c) Hesse, C.; Leroy, N.; Roncln, J. *Mol. Phys.* **1971**, *22*, 137. (d) Michaut, J. P.; Roncin, J. *Chem. Phys. Lett.* **1971**, *12*, 95. (e) Maas, G.; Maltsen, A. A.; Margrave, J. L. *J. Inorg. Nucl. Chem.* **1973**, *35*, 1945. (f) Legett, T. L.; Kohl, D. A. *J. Chem. Phys.* **1973**, *59*, 611.

Table X. MNDO, HF/3-21G, and HF/6-31G* Optimized and Relative Energies of All Equilibrium and Transition Structures

	MNDO		HF/3-21G		HF/6-31G*	
molecule	energy[a]	R.E.[b]	energy[c]	R.E.[b]	energy[c]	R.E.[b]
CHF_2 (C_s)	-89.5	0.0	-235.979 24	0.0	-237.263 13	0.0
CHF_2 (C_{2v})	-89.4	0.1	-235.968 47	6.8	-237.247 17	10.0
CF_3 (C_{3v})	-138.7	0.0	-334.313 36	0.0	-336.131 18	0.0
CF_3 (D_{3h})	-131.2	7.5	-334.271 39	26.3	-336.078 59	33.0
$CHCl_2$ (C_s)			-952.754 01	0.0	-957.358 05	0.0
$CHCl_2$ (C_{2v})	3.0	0.0	-952.752 11	1.2	-9579.356 54	0.9
CCl_3 (C_{3v})			-1409.450 42	0.0	-1416.248 16	0.0
CCl_3 (D_{3h})	-0.6	0.0	-1409.447 07	2.1	-1416.245 39	1.7
CHFCl (C_1)			-594.360 07	0.0	-597.306 23	0.0
CHFCl (C_s)	-41.7	0.0	-594.353 63	4.0	-597.299 32	4.3
CF_2Cl (C_s)	-90.1	0.0	-692.680 45	0.0	-696.163 29	0.0
CF_2Cl (C_{2v})	-86.5	3.6	-692.655 35	15.8	-696.134 85	17.8
$CFCl_2$ (C_s)	-43.2	0.0	-1051.058 11	0.0	-1056.201 59	0.0
$CFCl_2$ (C_{2v})	-42.4	0.8	-1051.045 92	7.6	-1056.189 34	7.7

[a] MNDO energies (heats of formation) are in kcal/mol. [b] Energy differences are in kcal/mol. [c] Energy is in hartrees.

Table XI. Ranges of $\Delta H_f°_0(CH_3F)$ as Determined by the Heat of Formation of Each Species Listed in the Last Column of Table I, and Their Intersections[a]

species	$\Delta H_f°_0(CH_3F)$	intersection
CH_2F	-49.1 to -57.1	-49.1 to -57.1
CHF_2	-51.05 to -55.05	-51.05 to -55.05
CF_3	-49.8 to -52.4	-51.05 to -52.4
CH_3F	-51.0 to -56.8	-51.05 to -52.4
CH_2F_2	-50.4 to -54.0	-51.05 to -52.4
CHF_3	-48.95 to -51.55	-51.05 to -51.55
CF_4	-48.05 to -50.05	

[a] Values are in kcal/mol.

Table XII. Ranges of $\Delta H_f°_0(CH_3Cl)$ as Determined by the Heat of Formation of Each Species Listed in the Last Column of Table I, and Their Intersections[a]

species	$\Delta H_f°_0(CH_3F)$	intersection
CH_2Cl	-13.5 to -20.6	-13.5 to -20.6
$CHCl_2$	-14.65 to -17.55	-14.65 to -17.55
CCl_3	-15.69 to -19.35	-15.69 to -17.55
CH_3Cl	-16.4 to -19.1	-16.4 to -17.55
CH_2Cl_2	-15.0 to -18.4	-16.4 to -17.55
$CHCl_3$	-15.4 to -17.0	-16.4 to -17.0
CCl_4	-14.99 to -16.69	-16.4 to -16.69

[a] Values are in kcal/mol.

the HF/3-21G and HF/6-31G* level of calculation, though the inversion barrier is found to be slightly higher in CCl_3. If the more accurate results for CH_2Cl also apply to CCl_3, then an experimentally determined inversion barrier for this radical may be less than 1.7 kcal/mol. There is a definite contraction in the C–Cl separation when the molecule becomes planar, as opposed to the negligible change in the C–F bond length found in CF_3.

For the series CH_3, CH_2Cl, $CHCl_2$, and CCl_3, there is a monotonic increase in the inversion barrier at the HF/3-21G and HF/6-31G* levels, while the MNDO method produces planar equilibrium structures for all members.

It is clear from the molecules discussed above that fluorine destabilizes a planar geometry more than chlorine. Therefore, CHFCl is expected to be more nonplanar than $CHCl_2$ and more planar than CHF_2. Similarly, the inversion barrier in CF_2Cl should lie between that of $CFCl_2$ and CF_3, while $CFCl_2$ should be between CHFCl or CCl_3 and CF_2Cl. These predictions are supported by the calculated geometries (β values) and inversion barriers at all levels.

The ranges of $\Delta H_f°_0(CH_3F)$ as determined from each fluorinated methane and methyl radical are presented in Table XI. For example, since the calculated energy change for the reaction

$$CH_3 + CH_3F \rightarrow CH_4 + CH_2F$$

is -3.5 ± 2.0 kcal/mol and the experimental $\Delta H_f°_0(CH_2F) = -7.0$ ± 2.0 kcal/mol, the heat of formation of CH_3F can be between -49.1 and -57.1 kcal/mol. Continuing this procedure for all other species and taking the intersection of the ranges, we find that for all species except CF_4 the heat of formation of CH_3F can lie between -51.05 and -51.55 kcal/mol. The range of values calculated for CF_4 lies outside the ranges determined by CHF_2, CH_3F, and CH_2F_2. Performing a similar analysis for the heat of formation of CH_3Cl (Table XII) shows that all reactions are satisfied for a $\Delta H_f°_0(CH_3Cl)$ value between -16.4 and -16.69 kcal/mol,

Taking the heats of formation of CH_3F and CH_3Cl as -51.3 ± 0.3 and -16.6 ± 0.2 kcal/mol, respectively, and calculated reaction energies that have an uncertainty of 2.0 kcal/mol, the heats of formation of all other species are calculated. For the chlorofluoromethanes and methyl radicals, we use the following homodesmic reactions;

$$CH_3 + nCH_3F + mCH_3Cl \rightarrow (n + m)CH_4 + CH_{3-n-m}F_nCl_m$$

$$nCH_3F + mCH_3Cl \rightarrow (n + m - 1)CH_4 + CH_{4-n-m}F_nCl_m$$

These MP2/6-31G*//HF/3-21G heats of formation at 0 and 298 K are presented in Table XIII. Experimental conversions between these temperatures are used for all halomethanes, while standard

Table XIII. MP2/6-31G*//HF/3-21G Heats of Formation of Halogenated Methyl Radicals and Methanes[a]

species	$\Delta H_f°_0$	$\Delta H_f°_{298}$
CH_2F	-3.2 ± 2.3	-4.0 ± 2.3
CHF_2	-55.1 ± 2.6	-55.7 ± 2.6
CF_3	-113.2 ± 2.9	-113.8 ± 2.9
CH_2Cl	31.7 ± 2.2	31.0 ± 2.2
$CHCl_2$	25.3 ± 2.4	24.8 ± 2.4
CCl_3	20.4 ± 2.6	20.5 ± 2.6
CHFCl	-11.5 ± 2.5	-12.1 ± 2.5
CF_2Cl	-64.8 ± 2.8	-65.2 ± 2.8
$CFCl_2$	-20.4 ± 2.7	-20.7 ± 2.7
CH_3F	-51.3 ± 2.3	-53.3 ± 2.3
CH_2F_2	-103.8 ± 2.6	-105.6 ± 2.6
CHF_3	-167.1 ± 2.9	-168.8 ± 2.9
CF_4	-229.6 ± 3.2	-231.0 ± 3.2
CH_3Cl	-16.6 ± 2.2	-18.5 ± 2.2
CH_2Cl_2	-20.7 ± 2.4	-22.3 ± 2.4
$CHCl_3$	-24.6 ± 2.6	-25.8 ± 2.6
CCl_4	-26.3 ± 2.8	-26.8 ± 2.8
CH_2FCl	-58.7 ± 2.5	-60.4 ± 2.5
CHF_2Cl	-113.7 ± 2.8	-115.2 ± 2.8
$CHFCl_2$	-66.9 ± 2.7	-68.2 ± 2.7
CF_3Cl	-174.7 ± 3.1	-175.9 ± 3.1
CF_2Cl_2	-121.6 ± 3.0	-122.6 ± 3.0
$CFCl_3$	-72.1 ± 2.9	-72.9 ± 2.9

[a] Heats of formation are in kcal/mol.

Table XIV. Calculated in C-H Bond Strengths in Halogenated Methanes[a]

molecule	D(C-H)	molecule	D(C-H)
CH_3F	101.4	$CHCl_3$	97.2
CH_2F_2	102.0	CH_2FCl	100.4
CHF_3	107.1	CHF_2Cl	102.1
CH_3Cl	101.6	$CHFCl_2$	100.1
CH_2Cl_2	99.2		

thermochemical formulas[68] and the scaled HF/3-21G frequencies are used for the halogenated methyl radicals. Since any homodesmic reaction producing CH_3F or CH_3Cl will have an uncertainty of 2 kcal/mol, the uncertainties in the heats of formation for these molecules is increased to 2.3 and 2.2 kcal/mol, respectively.

The MP2/6-31G*//HF/3-21G heats of formation (Table XIII) are generally in good agreement with the experimental values listed in Table I. The calculated $\Delta H_f°_0$ of CH_2F and CHF_2 are above the experimental values, but they have overlapping error bars. The theoretical heat of formation of CF_3 is in better agreement with experiment and seems to support the later experimental value of -113.4 kcal/mol[70] more than the earlier values of -111.8[68] and -111.9 kcal/mol,[69] though all values are within the theoretical uncertainty. The calculated $\Delta H_f°_0$ values for CH_2Cl and $CHCl_2$ are in excellent agreement with experiment, while the value for CCl_3 definitely supports the earlier experimental heats of formation[68,69,71] more than the later value.[70] CF_2Cl has a theoretical heat of formation that is within the experimental error, while the experimental $\Delta H_f°_0(CFCl_2)$ is within the calculated range. These results predict $\Delta H_f°_0(CHFCl) = -11.5 \pm 2.5$ kcal/mol.

In general, the mono- and dihalomethanes have calculated heats of formation that are less negative than experiment while the tri- and tetrahalomethanes have calculated values that are more negative. The calculated value of $\Delta H_f°_0(CH_3F)$ supports the experimental value of -53 ± 2 kcal/mol,[69,75] but it has overlapping error bars with all values in Table I. All experimental values for the heat of formation of CH_2F_2 lie within the theoretical values, while only $\Delta H_f°_0(CHF_3) = -162.8$ kcal/mol[70] lies outside of the theoretical value. The calculated heats of formation of CH_3Cl, CH_2Cl_2, and $CHCl_3$ are all in good agreement with experiment; CCl_4 has a calculated heat of formation that agrees only with the most recent value of -24.1 kcal/mol.[70] CH_2FCl and $CHFCl_2$ have calculated heats of formation that are in very good agreement with the thermochemical estimate,[68] while the theoretical value of $\Delta H_f°_0(CHF_2Cl)$ argues against the earlier value of -118.4 kcal/mol.[72] The calculated heats of formation of CF_3Cl, CF_2Cl_2, and $CFCl_3$ support the more negative $\Delta H_f°_0$ values in Table I and have a significant disparity with the values presented in the 1982 compendium.[70]

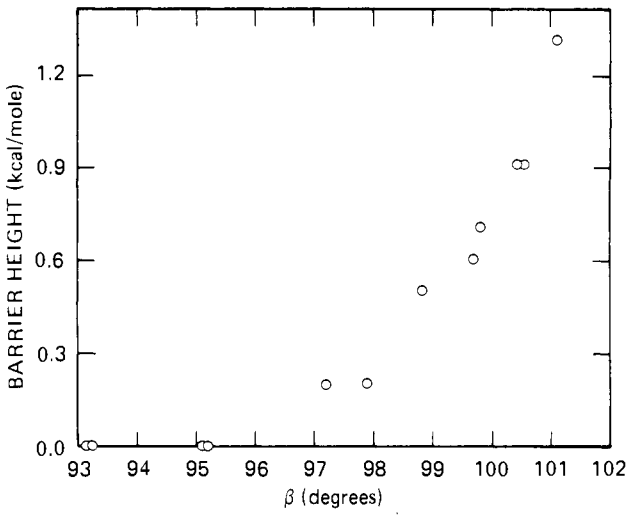

Figure 2. Plot of the inversion barrier without zero-point energy correction (kcal/mol) vs. the degree of nonplanarity (β value) for CH_2F and CH_2Cl at all ab initio levels of optimization in Tables III and VI.

With use of the $\Delta H_f°_{298}$ values listed in Table XIII and the known heat of formation of atomic hydrogen,[73] the C-H bond strengths of the halogenated methanes are presented in Table XIV. These values can be compared with a C-H bond strength in methane of 104.8 kcal/mol. This table shows that the C-H bond in halogenated methanes becomes stronger as more fluorines are present and weaker if more chlorines are present.

Discussion

From the optimized equilibrium structures and the calculated inversion barriers, the degree of nonplanarity and the inversion barrier for substituted methyl radicals increases in the substituent order H < Cl < F. Only CH_3 is found to have a planar equilibrium geometry at the HF/3-21G and HF/6-31G* levels of theory.

The HF/3-21G calculations predict a more planar structure for the fluorinated methyl radicals than do the HF/6-31G* results. For the chlorinated methyl radicals the reverse is true; the HF/3-21G optimized geometries are slightly more nonplanar than the HF/6-31G* structures. At the HF/3-21G and HF/6-31G* levels, the addition of halogens to CH_3 reduced the C-H separation, though this bond length was approximately the same for all halogenated methyl radicals. All methods agree in predicting a reduction in the C-H distance upon going from a nonplanar equilibrium geometry to a planar transition structure.

In most cases, the HF/6-31G* optimized C-Cl separation was found to be shorter than the MNDO bond length, while the HF/3-21G calculations yielded C-Cl distances which were substantially longer. The difference between the HF/6-31G* and HF/3-21G C-Cl bond length exceeded 0.1 Å in CH_2Cl. This separation was found to be the smallest in CCl_3 at both MNDO and HF/3-21G levels, and the longest in CF_2Cl at all levels. The

(68) Stull, D. R.; Prophet, H., Project Directors, *JANAF Thermochemical Tables*, 2nd ed.; U.S. Government Printing Office: Washington D.C., 1971; NSRDS-NBS 37.

(69) Benson, S. W. *Thermochemical Kinetics*; 2nd ed.; Wiley-Interscience: New York, 1976.

(70) Wagman, D. D.; Evans, W. H.; Parker, V. B.; Schumm, R. H.; Hallow, I.; Bailey, S. M.; Churney, K. L.; Nuttall, R. L. *J. Phys. Chem. Ref. Data* **1982**, *11*, Suppliment 2.

(71) Mendenhall, G. D.; Golden, D. M.; Benson, S. W. *J. Phys. Chem.* **1973**, *77*, 2707.

(72) Stull, D. R.; Westrum, E. F., Jr.; Sinke, G. C. *The Chemical Thermodynamics of Organic Compounds*; Wiley: New York, 1969.

(73) Chase, M. W., Curnutt, J. L.; Downey, J. R., Jr.; McDonald, R. A.; Syverud, A. N.; Valenzuela, E. A. *J. Phys. Chem. Ref. Data* **1982**, *11*, 695.

(74) Doering, W. V. E. *Proc. Natl. Acad. Sci. U.S.A.* **1981**, *78*, 5297.

(75) Benson, S. W. *Chem. Rev.* **1978**, *78*, 23.

(76) Benson, S. W. *J. Phys. Chem.* **1981**, *85*, 3375.

(77) Chase, M. W.; Curnutt, J. L.; Hu, A. T.; Prophet, H.; Syverud, A. N.; Walker, L. C. *J. Phys. Chem. Ref. Data* **1974**, *3*, 311.

(78) Benson, S. W.; O'Neal, H. E. *Kinetic Data on Gas Phase Unimolecular Reactions*; U.S. Government Printing Office: Washington D.C., 1970; NSRDS-NBS 21.

(79) Shaw, R. In *The Chemistry of the Functional Groups: The Chemistry of the Carbon Halogen Bond*; Patai, S., Ed.; Wiley: New York, 1973; Chapter 16.

(80) Pamidimukkala, K. M.; Rogers, D.; Skiner, B. *J. Phys. Chem. Ref. Data* **1982**, *11*, 83.

(81) McMillan, D. F.; Golden, D. M. *Annu. Rev. Phys. Chem.* **1982**, *33*, 493.

(82) Bassett, J. E.; Whittle, E. *J. Chem. Soc., Faraday Trans 1* **1972**, *68*, 492.

(83) Martin, J. P.; Paraskevopoulos, G. *Can. J. Chem.* **1983**, *61*, 861.

(84) Okabe, K. *J. Chem. Phys.* **1977**, *66*, 2058.

(85) DeCorpo, J. J.; Bafus, D. A.; Franklin, J. L. *J. Chem. Thermo.* **1971**, *3*, 125.

(86) Weissman, M.; Benson, S. W. *J. Phys. Chem.* **1983**, *87*, 243.

(87) Benson, S. W.; Weissman, M. *Int. J. Chem. Kinet.* **1982**, *14*, 1287.

(88) Foon, R.; Tait, K. B. *J. Chem. Soc., Faraday Trans. 1* **1972**, *68*, 104.

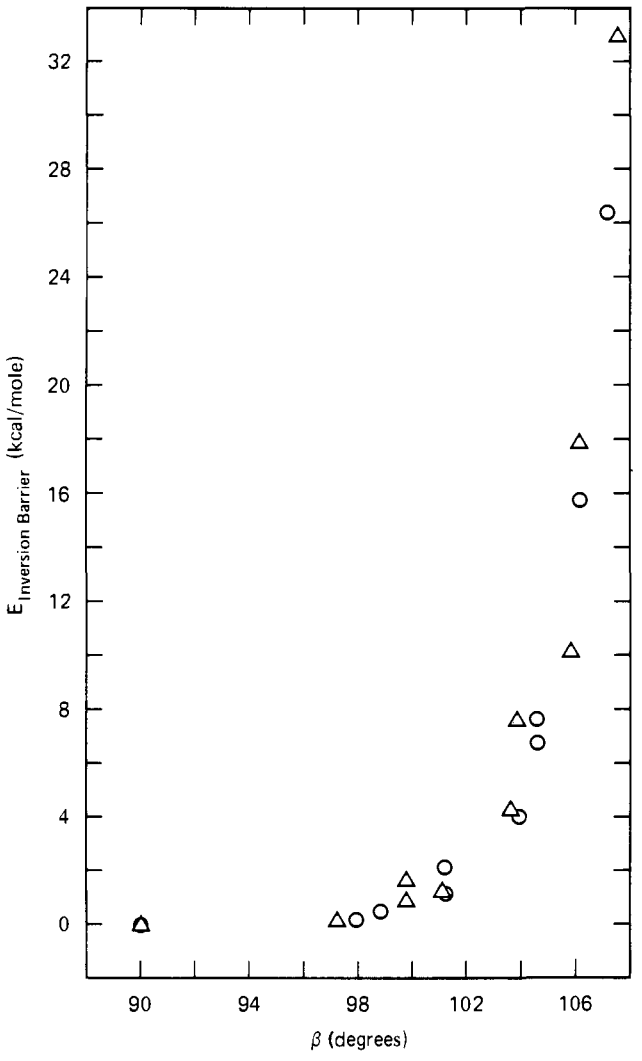

Figure 3. Plot of the inversion barrier without zero-point energy correction (kcal/mol) vs. with degree of nonplanarity (β value) for the halogenated methyl radicals at the HF/3-21G (○) and HF/6-31G* (△) levels of theory.

variation in the C–Cl distance for different molecules was found to be quite small at the HF/6-31G* level. All levels of calculation agree in predicting a decrease in the C–Cl separation upon becoming planar, and this variation was larger than that found in either the C–H or the C–F distances.

These results indicate a correlation between the degree of nonplanarity of the equilibrium structure and the resulting inversion barrier. To illustrate this correlation, Figure 2 shows a plot of the inversion barrier vs, the degree of nonplanarity (β value) for CH_2F and CH_2Cl at all levels of optimization presented in Tables III–VIII. A similar curve is shown in Figure 3 for all halomethyl radicals with use of the HF/3-21G and HF/6-31G* results. The resulting curves suggest that a functional relationship exists between the inversion barrier and degree of nonplanarity of the equilibrium structure and that this function is independent of the level of calculation. A good example of this is the HF/3-21G calculation on CH_2Cl and the HF/6-31G* results for CH_2F. These different levels of calculation for different molecules yield equilibrium structures with approximately the same degree of nonplanarity (the β values are 101.2° and 101.1°, respectively) and very similar inversion barriers. This suggests that if the value of β is known for the equilibrium geometry of a substituted methyl radical, the inversion barrier is also known without further calculations. As mentioned in the introduction, the addition of a second nonbonding electron on the central atom (substituted methyl anion) should increase the unfavorability of a planar structure and would not be expected to produce points that fall on this same curve.

Table XV. HF/3-21G*, HF/6-31G*, and MP2/6-31G*//HF/3-21G Atom Equivalents[a]

atom	HF/3-21G	HF/6-31G*	MP2/6-31G* //HF/3-21G
H–(C)	−0.56654[b]	−0.56967[b]	−0.57261
F–(C)	−98.81559[b]	−99.34989[b,c]	−99.51734
Cl–(C)	−457.26721	−459.46093	−459.58587
$C-(H)_3(R)$[d]	−37.68096[b]	−37.88935[b]	−38.01318
$C-(H)_2(R)_2$	−37.67842[b]	−37.88750[b]	−38.01416
$C-(H)(R)_3$	−37.67300[b]	−37.88371[b]	−38.01651
$C-(R)_4$	−37.66260	−37.87736	−38.01983
$^{\bullet}C-(H)_2(R)$[e]	−37.67898	−37.89742	−38.00652
$C-(H)(R)_2$	−37.69060	−37.90341	−38.01018
$^{\bullet}C-(R)_3$	−37.69696	−37.90513	−38.01106

[a] Atom equivalents are in hartrees. [b] Data from ref 89. [c] Correction of a typographical error in ref 89. [d] Value also used in CH_4. [e] Value also used for CH_3.

The results presented in Table XIV suggest that if the CF_3 radical were produced by anaerobic reductive metabolism, it could potentially abstract a hydrogen from virtually any carbon, even methane. At the other extreme, when CCl_3 is produced by the reductive metabolism of CCl_4, it can only abstract a lipid hydrogen if the C_L–H bond strength is less than about 97.2 kcal/mol. This value implies that the hydrogen would have to come from an unsaturated section of the lipid molecule, or from environments where the resulting carbon radical is stabilized. Between these extremes, there are definite trends in the strength of the carbon–hydrogen bond with halogen substitution. When hydrogens in methane are replaced by chlorines, there is a decrease in the C–H bond strength; the bond strength increases as more fluorines are present.

The theoretical heats of formation shown in Table XIII have argued against certain of the previously published values listed in Table I for CCl_3, CHF_3, CCl_4, CH_2FCl, CHF_2Cl, $CHFCl_2$, CF_3Cl, CF_2Cl_2, and $CFCl_3$. Removing these values from consideration reduces the spread in the experimental heats of formation for these species. These data can now be used to extend the list of atom equivalents presented by Ibrahim and Schleyer,[89] which allows for a direct determination of the heat of formation at 298 K from HF/3-21G and HF/6-31G* energies. In this earlier study, atom equivalents for H, C, N, O, and F were determined in various chemical environments. For a saturated carbon center, three different atom equivalents were determined, corresponding to $C-(H)_3(R)$, $C-(H)_2(R)_2$, and $C-(H)(R)_3$, where R is C, N, O, or F. Due to a lack of sufficient data, an atom equivalent for a quaternary carbon was not determined. In addition, a radical carbon was given a single atom equivalent value independent of its environment,

Assuming that chlorine can be treated as an R atom in this analysis, the data presented here can be used to determine the following atom equivalents: Cl–(C), $C-(R)_4$, $^{\bullet}C-(H)_2(R)$, $^{\bullet}C-(H)(R)_2$, and $^{\bullet}C(R)_3$ (R = F, Cl). For example, the experimental heats of formation, HF/3-21G, and HF/6-31G* energies of CH_3Cl, CH_2Cl_2, $CHCl_3$, CH_2FCl, CHF_2Cl, and $CHFCl_2$ can be used with Ibrahim and Schleyer's atom equivalents[89] to determine the Cl–(C) equivalent. Once this value is determined, the heat of formation and ab initio energy of CF_4, CCl_4, CF_3Cl, CF_2Cl_2, and $CFCl_3$ produce the $C-(R)_4$ equivalent. Following the groupings of Ibrahim and Schleyer, $^{\bullet}C-(H)_2(R)$ is determined from CH_3, CH_2F, and CH_2Cl; $^{\bullet}C-(H)(R)_2$ from CHF_2 and $CHCl_2$; and $C-(R)_3$ from CF_3, CCl_3, CF_2Cl, and $CFCl_2$. CHFCl cannot be used to determine $^{\bullet}C-(H)(R)_2$ since no experimental heat of formation is known. The resulting HF/3-21G and HF/6-31G* atom equivalents are listed in the second and third columns of Table XV, respectively,

The last column of this table lists equivalents for these atoms at the MP2/6-31G*//HF/3-21G level of theory. No values have been previously determined at this level, so all equivalents are

(89) Ibrahim, M. R.; Schleyer, P. v. R. *J. Comp. Chem.* **1985**, *6*, 157.

Table XVI. Heats of Formation (298 K) from Atom Equivalents[a]

species	HF/3-21G	HF/6-31G*	MP2/6-31G* //HF/3-21G	exptl[b]
CH_4	-18.7	-17.0	-18.1	-17.9
CH_3F	-53.8	-54.2	-54.6	-55.9
CH_2F_2	-104.4	-106.5	-106.3	-107.4
CHF_3	-166.6	-168.5	-166.7	-166.4
CF_4	-233.0	-231.1	-224.9	-222.0
CH_3Cl	-26.2	-21.2	-20.7	-19.65
CH_2Cl_2	-28.0	-22.9	-24.4	-22.47
$CHCl_3$	-27.0	-21.0	-25.6	-24.64
CCl_4	-25.4	-14.9	-22.8	-24.6
CH_2FCl	-62.4	-62.2	-61.8	-62.6
CHF_2Cl	-111.2	-114.7	-112.9	-113.7
$CHFCl_2$	-64.1	-65.4	-67.2	-67.7
CF_3Cl	-168.6	-172.7	-170.0	-169.1
CF_2Cl_2	-112.0	-116.5	-117.3	-117.75
$CFCl_3$	-63.9	-63.8	-68.1	-69.5
CH_3	22.6	29.8	35.0	34.8
CH_2F	-15.7	-9.7	-6.1	-7.8
CHF_2	-57.1	-56.6	-56.8	-59.2
CF_3	-106.4	-110.7	-113.5	-113.2
CH_2Cl	16.8	23.0	28.6	30.55
$CHCl_2$	23.7	23.1	23.3	25.7
CCl_3	30.2	24.9	17.9	18.75
CHFCl	-12.6	-14.0	-13.3	
CF_2Cl	-53.4	-61.2	-65.1	-64.3
$CFCl_2$	-7.0	-15.5	-21.0	-23.0

[a] Values are in kcal/mol. [b] Values from Table I corrected to 298 K.

simultaneously determined. Since C-(H)$_3$(R) is used for the carbon in methane[89] and •C-(H)$_2$(R) is chosen to represent the carbon in CH_3, these data are not sufficient to uniquely determine the atom equivalents. Any constant can be added to the H-(C), F-(C), and Cl-(C) values as long as four times this constant is subtracted from all carbon atom equivalents. To circumvent this problem, the MP2/6-31G*//HF/3-21G energy of ethane[90] and its heat of formation[89] are added to the set of equations used to determine the atom equivalents.

The resulting HF/3-21G, HF/6-31G*, and MP2/6-31G*//HF/3-21G heats of formation at 298 K are compared with experiment in Table XVI. For example, the theoretical heat of formation of CH_2FCl is obtained by taking the ab initio energy and subtracting C-(H)$_2$(R)$_2$, H-(C) twice, F-(C), and Cl-(C). Multiplying the result by 627.509 converts the heat of formation (298 K) from hartrees to kcal/mol. The average absolute errors between theory and experiment for these compounds are 5.6 kcal/mol at HF/3-21G, 3.5 kcal/mol at HF/6-31G*, and 1.2 kcal/mol at MP2/6-31G*//HF/3-21G. The excellent agreement between experiment and the MP2/6-31G*//HF/3-21G values is due to both the improved theoretical energy caused by adding electron correlation and the fact that only these data (and C_2H_6 to remove the additive constant) are used to determine the atom equivalents. It is interesting to note that the results in Tables XIII and XVI show that all theoretical heats of formation of CF_4 are significantly below experiment. Increasing the basis set and adding electron correlation decrease the error, but the MP2/6-31G*//HF/3-21G result in Table XVI is still too low by 2.9 kcal/mol. Since the experimental error bars are quite small for this compound (Table I), it appears to be necessary to go beyond the MP2 level to obtain an accurate heat of formation.

Acknowledgment. Support for this work from NIH Grant No. GM27943 is gratefully acknowledged.

(90) Whiteside, R. A.; Frisch, M. J.; Pople, J. A., Eds. *The Carnegie-Mellon Quantum Chemistry Archive*, 3rd ed.; Carnegie-Mellon University: Pittsburgh, 1983.

On the Mechanism of $(C,H_3,O)^{\cdot}$ Loss from Ionized Methyl Acetate. An ab Initio Molecular Orbital Study

Nikolaus Heinrich,[†] Jochen Schmidt,[†] Helmut Schwarz,*[†] and Yitzhak Apeloig[‡]

Contribution from the Institut für Organische Chemie der Technischen Universität, D-1000 Berlin 12, FRG, and the Department of Chemistry, Technion-Israel Institute of Technology, Haifa 32000, Israel. *Received July 24, 1986*

Abstract: Ab initio molecular orbital calculations executed at the MP2/6-31G(d)//3-21G level of theory and corrected for zero-point energies were used to provide insight into the gas-phase chemistry of ionized methyl acetate (**1**) and to resolve opposing interpretations of the experimental findings. The minimal energy requirement path has been located, and it is suggested that the experimentally observed dissociation of $CH_3CO_2CH_3^{\cdot+}$ (**1**) → $CH_3CO^+/CH_2OH^{\cdot}$ follows a multistep isomerization/dissociation pattern. In the first step, **1** isomerizes to the distonic ion $CH_3C(OH)OCH_2^{\cdot+}$ (**6**), which further rearranges to the hydrogen-bridged radical ion/dipole complex $CH_3CO\cdots H\cdots OCH_2^{\cdot+}$ (**8**). The latter, probably in its first excited state $^2(A'')$, is the direct precursor to the observed fragments $CH_3CO^+ + CH_2OH^{\cdot}$. The theoretical analysis provides a coherent description of the gas-phase ion chemistry of metastable **1**, which could not be achieved by the analysis of experimental data only. Semiempirical methods, like MNDO and MINDO/3, are less suited to describe the potential energy surface of ionized methyl acetate.

There is now ample experimental evidence that the $C_2H_3O^+$ ions generated from metastably dissociating molecular ions of methyl acetate (**1**) have the acetyl structure **2**.[1] The structure of the neutral fragment generated, the (C,H_3,O) radical, formed together with **2** in the dissociation of **1** (Scheme I) is, however, under dispute. The straightforward possibility is that the $(C,H_3,O)^{\cdot}$ radical is a methoxy radical, $CH_3O^{\cdot}$ (**3**). However, this suggestion has been revised recently[2a-e] by the claim that the

* To whom correspondence should be addressed.
† Institut für Organische Chemie der Technischen Universität.
‡ Israel Institute of Technology.

(1) (a) Schwarz, H.; Wesdemiotis, C. *Org. Mass Spectrom.* **1979**, *14*, 25. (b) Vajda, J. H.; Harrison, A. G.; Hirota, A.; McLafferty, F. W. *J. Am. Chem. Soc.* **1981**, *103*, 36. (c) Burgers, P. C.; Holmes, J. L.; Szulejko, J. E.; Mommers, A. A.; Terlouw, J. K. *Org. Mass Spectrom.* **1983**, *18*, 254. (d) Wesdemiotis, C.; Csenscits, R.; McLafferty, F W. *Org. Mass Spectrom.* **1985**, *20*, 98.

0002-7863/87/1509-1317$01.50/0